Phys Chem Minerals (2004) 31: 176–182
DOI 10.1007/s00269-004-0382-2

ORIGINAL PAPER

K. Saruwatari · J. Kameda · H. Tanaka

Generation of hydrogen ions and hydrogen gas in quartz–water crushing experiments: an example of chemical processes in active faults

Received: 26 June 2003 / Accepted: 26 December 2003

Abstract To understand the fundamental chemical processes of fluid–rock interaction during the pulverization of quartz grains in fault zones, quartz grains were crushed within pure water. The crushing experiments were performed batch style using a shaking apparatus. The crushing process induced a decrease in pH and an increase in hydrogen gas with increased shaking duration. The amount of hydrogen ions generated was five times larger than that of the hydrogen gas, which was consistent with the amount of Si radicals estimated from electron spin resonance measurements by Hochstrasser and Antonini (1972). This indicates that hydrogen gas was generated by consuming most of the Si radicals. The generation of hydrogen ions was most likely related to the presence of silanols on the newly formed mineral surface, implying a change of proton activities in the fluid after pulverization of quartz.

Keywords Hydrogen ion · Hydrogen gas · Quartz · Water · Crushing

Introduction

Chemical reactions, including fluid–rock interactions, are recognized as important in controlling the dynamic behavior and the deformation process of fault zones (Wintch et al. 1995; Stünitz and Tullis 2001). In the brittle regime, measurements of anomalous concentrations of gases and chemical elements along active faults provide evidence of water-rock interaction resulting from the pulverization of rocks (e.g. Wakita et al. 1980; Kennedy et al. 1997; Ito et al. 1999; Kharaka et al. 1999; Tanaka et al. 2001a). One of the characteristic products is hydrogen gas, which has been detected and associated with fault activities since Wakita et al. (1980) found hydrogen anomalies along an active fault with occurrence of earthquakes. Kita et al. (1982) performed experiments confirming that the hydrogen gas was generated by crushing quartz and granite under water-saturated conditions, and explained that the generation of hydrogen gas was due to the radical reaction between water molecules and active $\cdot Si\equiv$ sites on the new fracture surfaces of quartz. This phenomenon is related to the stress corrosion process proposed by Freiman (1984) (see Wakita 1994; Ito et al. 1999). Another characteristic product detected in the fault zone is submicron-sized low-strength materials, such as amorphous material and clays, which seem to be formed at disequilibrium conditions of temperature, pressure and fluid composition (Chester et al. 1993; Evans and Chester 1995; Tanaka et al. 2001a,b; Tanaka 2003). Mineral reactions that form clays from primary minerals generally progress with increase of hydrogen ion activities. Thus Tanaka (2003) considered whether hydrogen ions in fluids would be generated by activated crushed surfaces and confirmed, using a triaxial apparatus, that chemical reactions between crushed quartz and pure water produce hydrogen ions.

When the atomic bonds of SiO_2 are destroyed by grain crushing, two types of surface sites are produced (Fubini 1998): one is due to homolytic cleavage resulting in dangling bonds, $\equiv Si\cdot$ and $\equiv SiO\cdot$, which are detected using electron spin resonance (ESR) (Schrader et al. 1969; Hochstrasser and Antonini 1972); the other site is due to heterolytic cleavage that leads to surface charges, $\equiv Si^{+}$ and $^{-}O-Si\equiv$ (Fig. 1). Once these species are formed, they either recombine with each other to form siloxane bonds ($\equiv Si–O–Si\equiv$) or react with atmospheric components such as water molecules. According to the molecular dynamics simulations, the first of these processes is completed within a few picoseconds at ambient temperatures (Levine and Garofalini 1986; Koudriachova et al. 2000). Then, if water molecules are present, the

K. Saruwatari (✉) · J. Kameda · H. Tanaka
Department of Earth and Planetary Science,
University of Tokyo,
7-3-1 Hongo Bunkyo-ku Tokyo,
Japan 113–0033
E-mail: kazuko@eps.s.u-tokyo.ac.jp
Tel/Fax: +81-3-5841-4599

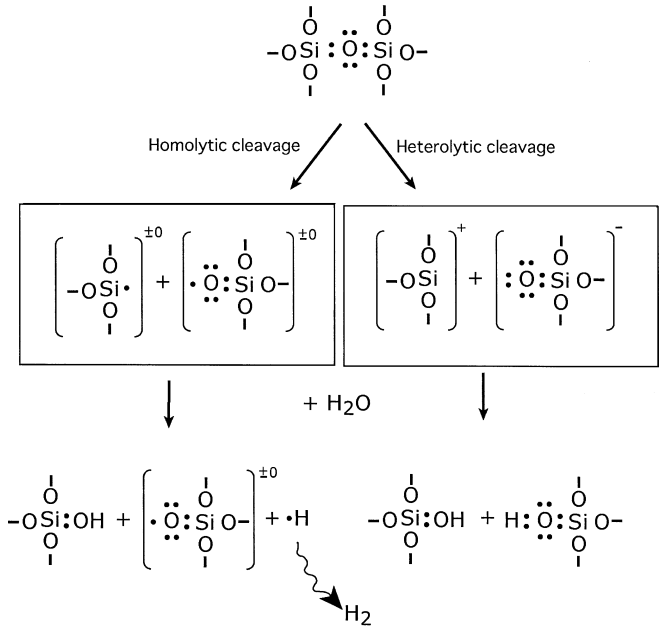

Fig. 1 Two types of bond breakage during quartz surface formation and reactions with water that follow at 25 °C

siloxane bonds react to form silanols (≡SiOH) (Levine and Garofalini 1986; D'Souza and Pantano 1999). The second of these processes also leads to reactions with water molecules to form silanols (Schrader et al. 1969):

$$\equiv \mathrm{Si}\cdot + \mathrm{H_2O} \rightarrow \equiv \mathrm{SiOH} + \mathrm{H}\cdot \quad (1)$$

$$\equiv \mathrm{SiO}\cdot + \mathrm{H}\cdot \rightarrow \equiv \mathrm{SiOH} \quad (2)$$

$$\equiv \mathrm{Si^{+}} + {}^{-}\mathrm{O} - \mathrm{Si} \equiv + \mathrm{H_2O} \rightarrow 2 \equiv \mathrm{SiOH} \ . \quad (3)$$

Because ≡SiO· is relatively stable up to 200 °C (Kita et al. 1982), reaction (2) is slower than reaction (1) at low temperatures. Thus the H· generated by reaction (1) is the most probable source of hydrogen gas by the reaction, $\mathrm{H}\cdot + \mathrm{H}\cdot \rightarrow \mathrm{H_2}\uparrow$ (Kita et al. 1982). However, the mechanism of the mechanochemical hydrogen ion formation has not been explained.

In this paper, we present procedure details and quantitative results of crushing experiments under argon-filled conditions at ambient temperature and pressure. The relationships among the generated hydrogen ions, hydrogen gas and the newly generated quartz surface areas are discussed.

Experimental procedure

Experiments were performed following methods of Kita et al. (1982) using a special ball mill (Fig. 2) made of alumina ceramic and a shaker, which moved the ball mill up and down with 50-mm amplitudes and 280 rpm (Miyamoto Riken MW-LWR) at room temperature (25 °C) and pressure. Alumina ceramic was used for the mill because of its rigidity and relatively low chemically reactivity with water. The volume of the mill is approximately 100 ml. Single crystals of Brazilian quartz were used as a starting material for the experiments. The crystals were crushed in an iron mortar and sieved, selecting the fraction between mesh sizes 0.15 and 0.512 mm. To purify the samples, a magnetic separator was used to remove iron fragments from the mortar and minor components such as opaque inclusion minerals in single crystals. Before the experiments were initiated, the purity of the samples was checked by X-ray diffraction, and the samples were washed in deionized and distilled water (hereafter referred to as pure water) using an ultrasonic cleaner until the water became clear. The pH of pure water (equal to 7.0 ± 0.1) was realized by bubbling the pure water with high-purity argon gas (99.995%) in a glove box (UNICO UN-650F), which was filled with the same high-purity argon gas and used in all the experiments. Five-g samples of quartz were combined with 15, 5 and 3 g of the pure water, referred to as 5/15, 5/5 and 5/3 samples, based on their quartz/water ratios. Each quartz sample immersed in pure water was crushed by moving a 1.5-cm-diameter alumina ball in the mill. Sample preparations and pH measurements were performed in a glove box to exclude oxygen and carbon dioxide to < 100 ppm and thus prevent oxidation of samples and water. After the crushing procedure, the fluid was separated into a polyethylene tube inside the glove box and then centrifuged before measuring pH. Gas samples were taken through a rubber septum, which was fixed within a Swagelok male connector (P-NPT-200–1-2) at the top of the mill using a gas-tight microsyringe.

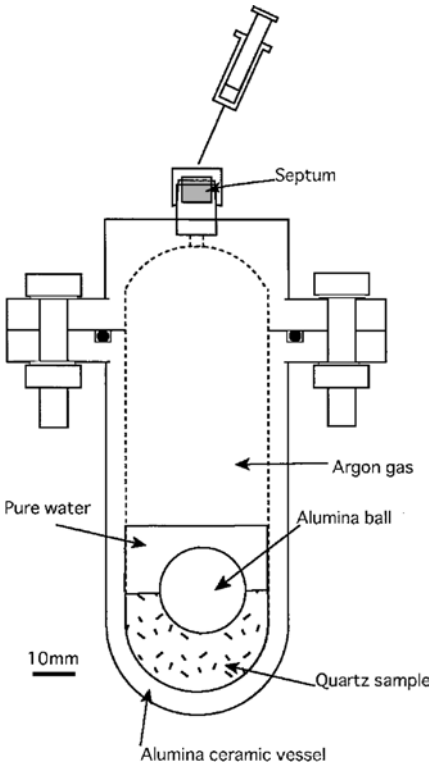

Fig. 2 Schematic drawing of crushing mill used in the experiments. Pure water (15 g, 5 g, 3 g), an alumina ball (1.5 cm in diameter) and quartz samples (5 g) are put together in the mill under an argon-filled condition. To take gas samples using a gas-tight microsyringe, a rubber septum is fixed within a Swagelok male connector at the top of the mill

Results

pH and hydrogen gas variations

pH was measured with an ORION 250 A pH meter and a Ross pH electrode connected to a personal computer.

Table 1 Experimental data of pH, H_2 and specific surface area for each quartz/water ratio examined

Qz/water	Duration (h)	pH	H_2 (ppm)	Surface area ($m^2\ g^{-1}$)
5 g/15 g	0.5	5.02	3.76	0.437
	1	4.73	6.33	0.563
	1.5	4.61	9.18	0.72
	2	4.6	13.31	0.859
5 g/5 g	0.5	4.52	3.00	0.433
	1	4.22	3.67	0.653
	1.5	4.14	5.07	0.917
	2	3.92	6.63	1.124
5 g/3 g	0.5	4.34	1.43	0.324
	1	4.12	3.37	0.596
	1.5	3.99	3.75	0.857
	2	3.75	5.92	1.087

The pH data were recorded at 5 s intervals. Experimental results show that pH decreases with increased shaking duration for all of the quartz/water ratio experiments (Table 1; Fig. 3a), indicating an increase in hydrogen ions. The decrease in pH is larger as the quartz/water ratio is decreased.

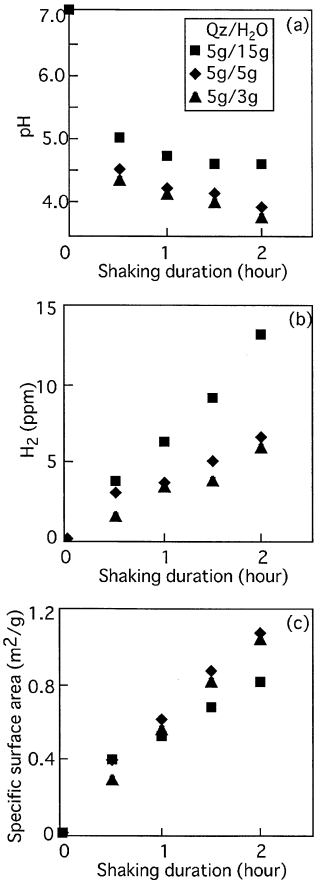

Fig. 3a–c Changes in pH (**a**), hydrogen gas (**b**), and specific surface area (**c**), as a function of shaking duration. Amounts of hydrogen gas and specific surface area increase with increased shaking durations, while pH decreases with increased shaking times

Hydrogen gas was measured by a gas chromatograph (Yanako G2700) with a column filled with molecular sieve 5 A and with using argon as a carrier gas. The amount of hydrogen gas also increased with as shaking duration was increased (Table 1; Fig. 3b). More hydrogen gas was generated with the 5/15 than the 5/5 and 5/3 quartz/water ratios. The amount of hydrogen gas measured was 1.3×10^{-9} to 1.1×10^{-8} mol per unit gram of quartz. The values are consistent with those observed by Kita et al. (1982) at room temperature.

Surface area of quartz

The Brunauer, Emmett and Teller (BET) method was adopted for precise measurements of the net surface area of crushed quartz grains (Brunauer et al. 1938; Adamson 1990). These measurements were performed with a Coulter SA 3100 Surface Area and Pore Size Analyzer using argon gas. The initial value of the net surface area ($0.038\ m^2g^{-1}$) corresponds to grain sizes between 0.5 and 0.15 mm (e.g. Rimstidt and Barnes 1980).

Following the crushing procedure, each sample was placed in a centrifuge at 5000 rpm for 20 min to remove the supernatant fluid, and then dried at 80 °C. The results show that net surface area increased with increased shaking duration (Table 1; Fig. 3c), corresponding to the introduction of finer grains generated by crushing. The results are consistent with the grain size reductions from experimental fragmentation and natural fault movements reported by Biegel et al. (1989) and Turcotte (1997).

Discussion

Mechanisms of hydrogen-gas and hydrogen-ion generation

The quantities of hydrogen atoms measured during the experiments, both hydrogen ions (H^+) and hydrogen gas ($H = 2 \times H_2$), are plotted against the new surface area (taking the difference between final and initial surface area measurements; Fig. 4). Amounts of both H^+ and H are approximately proportional to the newly formed surface area.

The quantities of H^+ and H per unit new surface area are 9×10^{-8} mol m^{-2} and $1–2 \times 10^{-8}$ mol m^{-2}, respectively. This implies that five to ten times as many H^+ ions are generated as H emitted in the form of hydrogen gas. In order to compare the amounts of both types of hydrogen with the number of broken Si–O bonds on the new surface, the total number of unsatisfied Si ligands on the new surface (N) is estimated from:

$$N = N_{Si} \cdot S = \left(\frac{N_A}{\upsilon_{SiO_2}}\right)^{2/3} \cdot S \ , \qquad (4)$$

where N_{Si} is the number of Si per unit surface, S is the total, newly formed surface area, N_A is Avogadro's

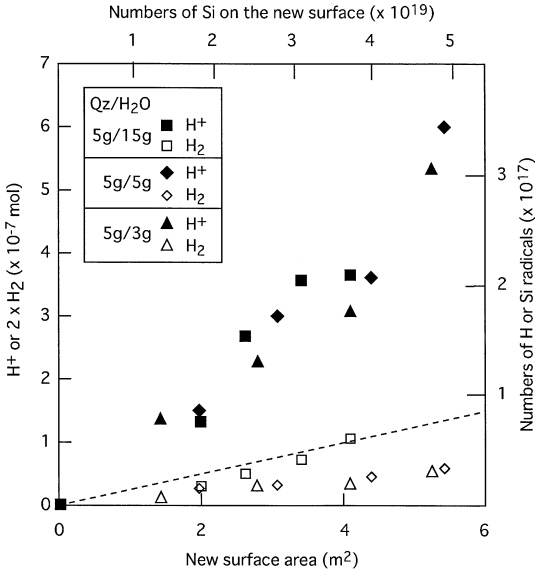

Fig. 4 Relationship between the generated hydrogen ions and hydrogen atoms of hydrogen gas to newly formed surface areas of quartz. The *upper X axis* displays the number of the unsatisfied Si bonds that is converted from the specific surface area. The *right side of the Y axis* shows the numbers of hydrogen atoms. A *dashed line* indicates a linear relationship between surface area and the numbers of Si radicals with the inclination of 1.4×10^{16} sp m^{-2}, which is obtained by the ESR measurements of Hochstrasser and Antonini (1972)

number and υ_{SiO_2} is the molar volume of the quartz (Tuel et al. 1990; D'Souza and Pantano 1999). Substituting 2.65 g cm^{-3} as the quartz density (Deer et al. 1992), N_{Si} is 8.9×10^{18} sites m^{-2}. Thus, the specific surface area is converted to the number of the unsatisfied Si bonds (shown on the upper *X* axis in the Fig. 4). The number of hydrogen atoms is displayed on the right side of the *Y* axis in the Fig. 4. The number of hydrogen ions and hydrogen atoms (in the form of H_2) is 0.6 and 0.1% of the unsatisfied Si ligands, respectively.

To quantify the contribution of Si radicals to the generation of H^+ and H, the number of Si radicals is estimated from the value of paramagnetic spin (1.4×10^{16} sp m^{-2}) determined by the ESR measurements of crushed quartz in ultra high vacuum (Hochstrasser and Antonini 1972). Assuming a linear relationship between the surface area and the number of Si radicals, we show, in Fig. 4, a dashed line constrained by the ESR measurements.

The number of Si radicals is generally consistent with the number of hydrogen atoms emitted as hydrogen gas, suggesting that the hydrogen gas is generated by consuming Si radicals. For the quartz/water ratio of 5/15, the amount of hydrogen in H_2 gas matches the number of Si radicals well. However, for the other quartz/water ratios, the amount of hydrogen in H_2 gas is less than the calculated numbers of Si radicals. The mismatch between the hydrogen gas produced and the Si radicals may be caused by the final pH of the water after crushing. According to quartz grinding experiments conducted by Kameda et al. (2003), the amount of hydrogen gas decreases with increased fluid acidity, especially below pH 5. These experiments suggest that the amount of hydrogen in H_2 gas also decreases with an increased quartz/water ratio, as the final pH of the water is decreased.

Research in the field of material sciences has found that interaction between H_2 and silicon interface results in the formation of mobile H^+ within silicon devices (e.g. Vanheusden et al. 1997; Lopez et al. 2000). According to the quantum-mechanical calculations of Lopez et al. (2000), H^+ will be generated due to H_2 dissociation initiated by reaction with Si dangling bonds, or by the reaction of atomic H with neutral O vacancies, if the electrons can be transferred into the Si conduction bands. However, in our experiments, H_2 exists only after reaction between water molecules and Si radicals, and the amount of H_2 is too small to react with other Si radicals. Furthermore, the experimental temperature is too low to complete the above reactions. Another concern is dissolved silica species that exist as monosilicic acid in solution. However, monosilicic acid is weak acid and a stable component only in alkaline solution (Dietzel 2000) with small dissociation constant $K = 10^{-9.71}$ (Faure 1991). Hence, dissolved silica species are unlikely to make pH decrease.

The formation of H^+, thus, is most likely related to the dissociation of surface silanols (≡SiOH), which are more strongly acid than monosilicic acid (e.g. Iler 1979) and generated from reactions between water molecules and the siloxane bonds after the reconstruction process or from reactions between water and the homolytic and hetelolytic disconnections of quartz (Fig. 1). The dissociation reaction is a 2-pK model with two consecutive reactions (and corresponding equilibrium constants):

$$\equiv SiOH_2^+ \Leftrightarrow \equiv SiOH + H^+ \tag{5}$$

$$K_1 = \frac{\{\equiv SiOH\} \cdot a_{H^+}}{\{\equiv SiOH_2^+\}} \tag{6}$$

$$\equiv SiOH \Leftrightarrow \equiv SiO^- + H^+ \tag{7}$$

$$K_2 = \frac{\{\equiv SiO^-\} \cdot a_{H^+}}{\{\equiv SiOH\}} \quad , \tag{8}$$

where $\{\equiv i\}$ stands for surface species *i* concentration, and a_{H+} is the hydrogen ion activity in solution. If it is assumed that the surface species are composed of ≡SiOH and $\equiv SiO^-$ ($\equiv SiOH_2^+$ is assumed to exist only at very low pH) and the equilibrium condition is attained instantly after crushing, so that $-\log_{10}K_2 = 7 \pm 1.0$ (as proposed by Hiemstra and Van Riemsdijk 1989 and Sahai and Sverjensky 1997), pH values with increasing surface silanols can be calculated from solving four simultaneous equations: Eq. (8), the dissociation equilibrium of water $[H^+][OH^-] = 10^{-14}$, electrical neutrality $V[H^+] = V[OH^-] + S\{\equiv SiO^-\}$ where *V* and *S* are solution volume and total surface area of quartz, respectively, and surface Si amounts

$\{\equiv SiOH\} + \{\equiv SiO^-\} = \alpha$ where α is estimated from BET surface area after experiments. Most of the experimental data are within the calculated pH range (Fig. 5), although experimental data with the larger quartz/water ratio gradually tend to deviate from the centre of the calculated pH range. From the above results and considerations, we conclude that hydrogen ion generation originates from the silanols on the new surface of crushed quartz grains.

Implications for active fault zones

Natural fault zones are marked by gouges that result from crushing processes and following alterations. Si radicals at the freshly produced silicate surfaces are expected to generate hydrogen gas, which may serve as an indicator of fault activity (e.g. Wakita et al. 1980; Sugisaki et al. 1983; Ito et al. 1999). Some of the hydrogen gas generated may remain in the fracture zone. Hydrogen gas concentrations have been observed to increase closer to the fracture zone in the core recovered from the Nojima fault, which was activated during the 1995 Kobe earthquake, Japan (Arai et al. 2001).

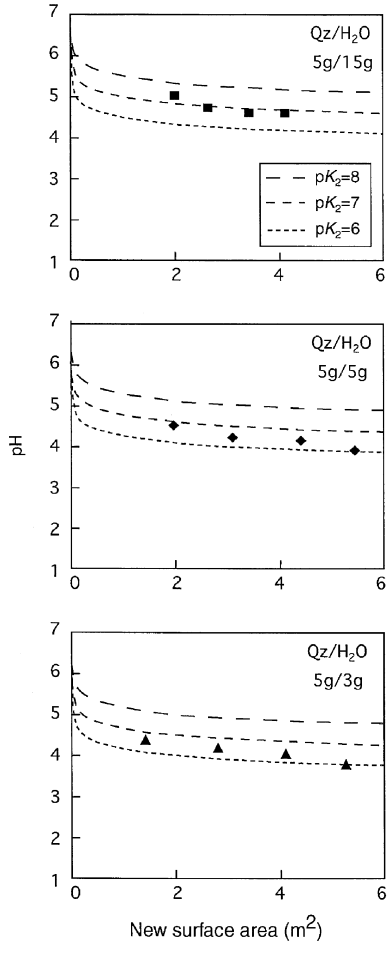

Fig. 5 Comparison between experimental determinations of pH and pH calculated by dissociation equilibrium of silanols for different values of the equilibrium constant ($pK = -\log_{10}K_2 = 6$, 7 and 8) assuming complete silanol formation at the new surface

Analyses of mineral assemblages in fault zones show that mafic minerals, including chlorite, are commonly depleted and altered to newly recrystallized clay minerals such as smectites (e.g. Chester et al. 1993; Ohtani et al. 2000; Tanaka et al. 2001b). One of the reactions that form smectite (Mg-monmorillonite) and consume chlorite in the presence of hydrogen ions is as follows:

$$1.165Mg_5Al_2Si_3O_{10}(OH)_8 + 0.175SiO_2(\text{amorph.}) + 11.316H^+ \rightarrow [Al_{2.00}(Si_{3.67}Al_{0.33})O_{10}(OH)_2]Mg_{0.167} + 6.658Mg^{2+} + 9.32H_2O \quad (9)$$

(e.g. Faure 1991).

Smectites have extremely low frictional strengths under water-saturated conditions (Byerlee 1978; Wang and Mao 1979; Logan and Rauenzahn 1987). Therefore, if the formation of smectite is accelerated by the increase of hydrogen ions during coseismic rupturing, the fault zone will be significantly weakened relative to the host rocks (Chester et al. 1993; Evans and Chester 1995; Wintsch et al. 1995; Tanaka et al. 2001b). During interseismic periods, precipitation of clay minerals and compaction may seal the gouge, which may play an important role in generating high pore fluid pressure within the fault zone (Olsen et al. 1998; Tenthorey et al. 2003). Thus, the presence of hydrogen ions, which can potentially promote the fluid–rock interactions in fault zones, affects the mechanical and transport properties governing seismic activity.

Previously, hydrogen ions were considered to have a meteoric origin (Wintsch et al. 1995; Tanaka et al. 2001b). Our experimental results show that the newly formed surface silanols may be a possible source of hydrogen ions, influencing the fluids that react with surrounding rocks of the fault zone. However, natural fault zones are not simplified as fracture zones composed of single crystals of quartz. In the case of rocks composed of other silicates, cations released during fracture will affect fluid composition and pH further. The fluid composition becomes more basic (Saruwatari et al. 2003), but silanols are probably formed on the new fractured surface of quartz, supplying hydrogen ions and leading to an exchange with the cations. Our experimental results and the reactions provide an example of the more complicated reactions between silicates and fluids that may occur in fault zones.

Conclusions

New surfaces of quartz produced by grain crushing generate hydrogen ions and hydrogen gas in adjacent fluids. Hydrogen ions evolved in this manner have concentrations five to ten times greater than hydrogen in the form of hydrogen gas, consistent with previous ESR spin determinations of concentration. Thus, the

hydrogen gas is most likely generated by Si radicals, while the hydrogen ions may be related to silanols at the new surface. The hydrogen gas and hydrogen ions are thus expected as products of crushing and gouge formation during seismic rupture of fault zones. Hydrogen ions may facilitate further chemical reaction of fluids with fault rocks to form weaker clay minerals.

Acknowledgements We very much appreciate A. Kronenberg and anonymous reviewers for their reviews and M. Akaogi for the editorial guidance. This research is supported by the Grants-in-Aid for Scientific Research System of the Japan Society for the Promotion of Science (13440134) and by a grant for a comprehensive research program on flow and slip processes in and below seismogenic regions, sponsored by the Ministry of Education, Culture, Sports, Science, and Technology, Japan.

References

Adamson AW (1990) Physical chemistry of surfaces, 5th edn. Wiley, New York, pp 777

Arai T, Okusawa T, Tsukahara H (2001) Behavior of gases in the Nojima fault zone revealed from the chemical composition and carbon isotope ratio of gases extracted from DPRI 1800 m drill core. Island Arc 10: 430–438

Biegel RL, Sammis CG, Dieterich JH (1989) The frictional properties of a simulated gouge having a fractal particle distribution. J Struct Geol 11: 827–846

Brunauer S, Emmett PH, Teller E (1938) Adsorption of gases in multimolecular layers. J Am Chem Soc 60: 309–319

Byerlee JD (1978) Friction of rocks. Pure Appl Geophys 116: 615–626

Chester FM, Evans JP, Biegel RJ (1993) Internal structure and weakening mechanisms of the San Andreas Fault. J Geophys Res 91: 771–789

Deer WA, Howie RA, Zussman J (1992) An introduction to the rock-forming minerals, 2nd edn. Longman, London, pp 696

Dietzel M (2000) Dissolution of silicates and the stability of polysilicic acid. Geochim Cosmochim Acta 64: 3275–3281

D'Souza A, Pantano CG (1999) Mechanisms for silanol formation on amorphous silica facture surfaces. J Am Ceram Soc 82: 1289–1293

Evans JP, Chester FM (1995) Fluid–rock interaction in faults of the San Andreas system: influences from San Gabriel fault-rock geochemistry and microstructures. J Geophys Res 100: 13007–13020

Faure G (1991) Principles and applications of inorganic geochemistry, 2nd edn. Prentice-Hall, London, pp 600

Freiman SW (1984) Effects of chemical environments on slow crack growth in glasses and ceramics. J Geophys Res 89: 4072–4076

Fubini B (1998) Health effects of silica. In: Legrand AP (ed) The surface properties of silicas. Wiley, New York, pp 415–464

Hiemstra T, Dewit JCM, Van Riemsdijk WHJ (1989) Multisite proton adsorption modeling at the solid/solution interface pf (hydr)oxides: a new approach II. Applications to various important (hyd)oxides. J Colloid Interf Sci 133: 105–117

Hochstrasser G, Antonini JF (1972) Surface states of pristine silica surfaces I. ESR studies of Es, dangling bonds and of CO_2-adsorbed radicals. Surface Sci 32: 644–664

Iler RK (1979) The chemistry of silica: solubility, polymerization, colloid and surface properties, and biochemistry, 1st edn. Wiley, New York, pp 866

Ito T, Nagamine K, Yamamoto K, Adachi M, Kawabe I (1999) Preseismic hydrogen gas anomalies caused by stress-corrosion process preceding an earthquake. Geophys Res Lett 26: 2009–2012

Kameda J, Saruwatari K, Tanaka H (2003) Hydrogen generation by wet grinding of quartz powders and its dependence on the pH and ionic strength of liquid media. Bull Chem Soc Jpn 76: 2153–2154

Kennedy BM, Kharaka YK, Evans WC, Ellwood A, DePaolo DJ, Thordsen J, Ambats G, Mariner RH (1997) Mantle fluids in the San Andreas fault system, California. Science 278: 1278–1280

Kharaka YK, Thorden JJ, Evans WC, Kennedy BM (1999) Geochemistry and hydrothermal interactions of fluids associated with the San Andreas fault system, California. Geophys Mono 113: 129–148

Kita I, Matuo S, Wakita H (1982) H_2 generation by reaction between H_2O and crushed rock: an experimental study on H_2 degassing from the active fault zone. J Geophys Res 87: 10789–10795

Koudriachova MV, Beckers JVL, de Leeuw SW (2000) Comparison of ab initio and empirical approaches to the quartz surface. Comput Mater Sci 20: 381–386

Levine SM, Garofalini SH (1986) Surface structure of silica glasses by molecular dynamics simulations. In: Galeener FL, Griscom DL, Weber MJ (eds) Defects in glasses. Proceeding of the Materials Research Society Symposium, vol. 61. Material Research Society, Pittsburgh, pp 28–37

Logan JM, Rauenzahn KA (1987) Frictional dependence of gouge mixtures of quartz and montmorillonite on velocity, composition and fabric. Tectonophysics 144: 87–108

Lopez N, Illas F, Pacchioni G (2000) Mechanisms of proton formation from interaction of H_2 with E, and oxygen vacancy centers in SiO_2: cluster model calculations. J Phys Chem 104: 5471–5477

Ohtani T, Fujimoto K, Ito H, Tanaka H, Tomida N, Higuchi T (2000) Fault rocks and past to recent fluid characteristics from the borehole survey of the Nojima fault ruptured in the 1995 Kobe earthquake, southwest Japan. J Geophys Res 105: 16161–16171

Olsen MP, Scholz CH, Leger A (1998) Healing and sealing of a simulated fault gouge under hydrothermal conditions: implications for fault healing. J Geophys Res 103: 7421–7430

Rimstidt JD, Barnes HL (1980) The kinetics of silica–water reactions. Geochim Cosmochim Acta 44: 1683–1699

Saruwatari K, Kameda J, Tanaka H (2003) Free-radical reactions by mechano-chemical process within seismic fault zones: results from fundamental experiments. Jpn Earth Plant Sci Joint meeting abstract

Sahai N, Sverjensky DA (1997) Evaluation of internally consistent parameters for the triple-layer model by the systematic analysis of oxide surface titration data. Geochim Cosmochim Acta 14: 2801–2826

Schrader R, Wissing R, Kubsch H (1969) Zur Oberflachenchemie von mechanisch activiertem Quartz. Z Anorg Allg Chem 365: 191–198

Sugisaki R, Ido M, Takeda H, Isobe Y, Hayashi Y, Nakamura N, Satake H, Mizutani Y (1983) Origin of hydrogen and carbon dioxide in fault gases and its relation to fault activity. J Geol 91: 239–258

Stünitz H, Tullis J (2001) Weakening and strain localization produced by syn-deformational reaction of plagioclase. Int J Earth Sci 90: 136–148

Tanaka H (2003) Hydrogen ion generation related with water-saturated pulverization of quartz, seismological radical reactions. In: Kasahara J, Toriumi M, Kawamura K (eds) The role of water in earthquake generation. Univ Tokyo Press, Tokyo, pp 208–209

Tanaka H, Fujimoto K, Ohtani T, Ito H (2001a) Structural and chemical characterization of shear zone in the freshly activated Nojima fault, Awaji Island, southwest Japan. J Geophys Res 106: 8789–8810

Tanaka H, Hinoki S, Kosaka K, Lin A, Tamkemura K, Murata A, Miyata T (2001b) Deformation mechanisms and fluid behavior in a shallow, brittle fault zone during co-seismic and interseismic periods: results from drill core penetrating the Nojima fault. Island Arc 10: 381–391

Tenthorey E, Cox SF, Todd HF (2003) Evolution of strength recovery and permeability during fluid–rock reaction in experimental fault zones. Earth Planet Sci Lett 206: 161–172

Tuel A, Hommel H, Legrand AP (1990) A ^{29}Si NMR study of the silanol population at the surface of derivatized silica. Langmuir 6: 770–775

Turcotte DL (1997) Fractals and chaos in geology and geophysics, 2nd edn. Cambridge University press, New York, pp 398

Vanheusden K, Warren WL, Devine RAB, Fleetwood DM, Schwank JR, Schaneyfelt MR,

Wakita H (1994) Subsurface gas behavior in active fault zones. In: Shimazaki K, Matsuda T (eds) Earthquakes and faults. Univ Tokyo Press, Tokyo, pp 173–187

Wakita H, Nakamura Y, Kita I, Fujii N, Notsu K (1980) Hydrogen release: new indicator of fault activity. Science 210: 188–190

Wang C, Mao N (1979) Shearing of saturated clays in rock joints at high confining pressures. Geophys Res Lett 6: 825–828

Wintsch RP, Christoffersen R, Kronenberg AK (1995) Fluid–rock reaction weakening of fault zones. J Geophys Res 100: 13021–13032